Engineering Conferences International
ECI Digital Archives

Fluidization XV | Proceedings

5-23-2016

Attrition rate of iron ore in the gas-solid fluidized beds with the wide size distribution

Dong-Hyun Kang
Department of Chemical Engineering, Sungkyunkwan University, Republic of Korea, dhlee@skku.edu

Chang Kuk Ko
Ironmaking Research Group, Technical Research Laboratories, POSCO, Republic of Korea

Dong Hyun Lee
Department of Chemical Engineering, Sungkyunkwan University, Republic of Korea

Recommended Citation
Dong-Hyun Kang, Chang Kuk Ko, and Dong Hyun Lee, "Attrition rate of iron ore in the gas-solid fluidized beds with the wide size distribution" in "Fluidization XV", Jamal Chaouki, Ecole Polytechnique de Montreal, Canada Franco Berruti, Wewstern University, Canada Xiaotao Bi, UBC, Canada Ray Cocco, PSRI Inc. USA Eds, ECI Symposium Series, (2016). http://dc.engconfintl.org/fluidization_xv/3

Fluidization XV

May 23, 2016

Attrition characteristics of iron ore by air jet in gas-solid fluidized beds

Dong Hyun Kang[1], Chang Kuk Ko[2], Dong Hyun Lee[1]*

Department of Chemical Engineering, Sungkyunkwan University, Republic of Korea[1]

Ironmaking Research Group, Technical Research Laboratories, POSCO, Republic of Korea[2]

*dhlee@skku.edu

SUNG KYUN KWAN UNIVERSITY

Contents

1. Introduction
2. Theory
3. Objective
4. Experiment
5. Result and discussion
6. Conclusion

SUNG KYUN KWAN UNIVERSITY

1. Introduction-1

• **Particle attrition in common process (Circulating Fluidized Bed Combustor)**

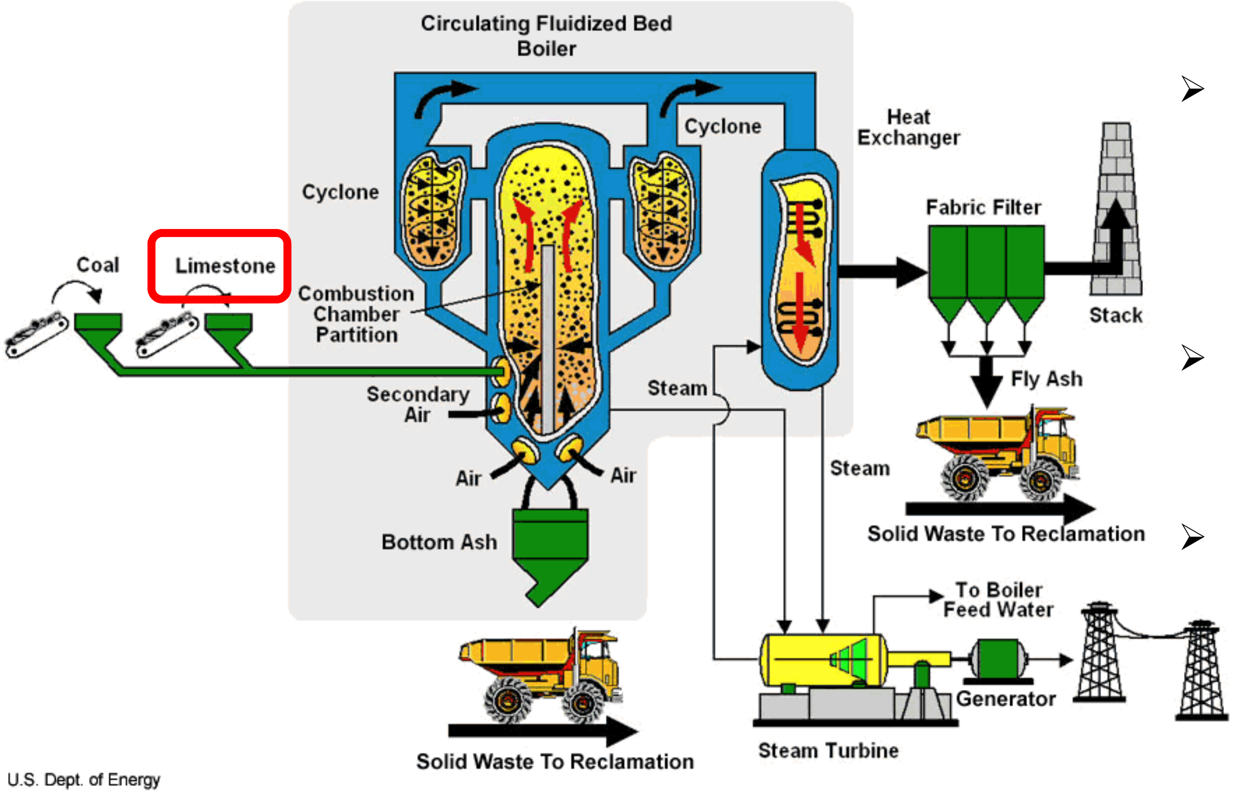

Fig. Typical Circulating Fluidized Bed Combustor (CFBC)
http://www.amrclearinghouse.org/Sub/landreclamation/cfb/wpcamr-cfbpower.htm

- Recent and future thermal power plant:

  Circulating Fluidized Bed Combustor

  Integrated Gasification Combined Cycle

- Limestone: absorbent of CO_2 and sulfur

  (severe condition of CFB reactor)

- Attrition studies of the limestone progressed

  Jia *et al*. (2007); Montagnaro *et al*. (2010)

  Xiao *et al*. (2011); Knight *et al*. (2014)

SUNGKYUNKWAN UNIVERSITY

1. Introduction-2

• **Particle attrition in FINEX fluidized bed reduction reactor**

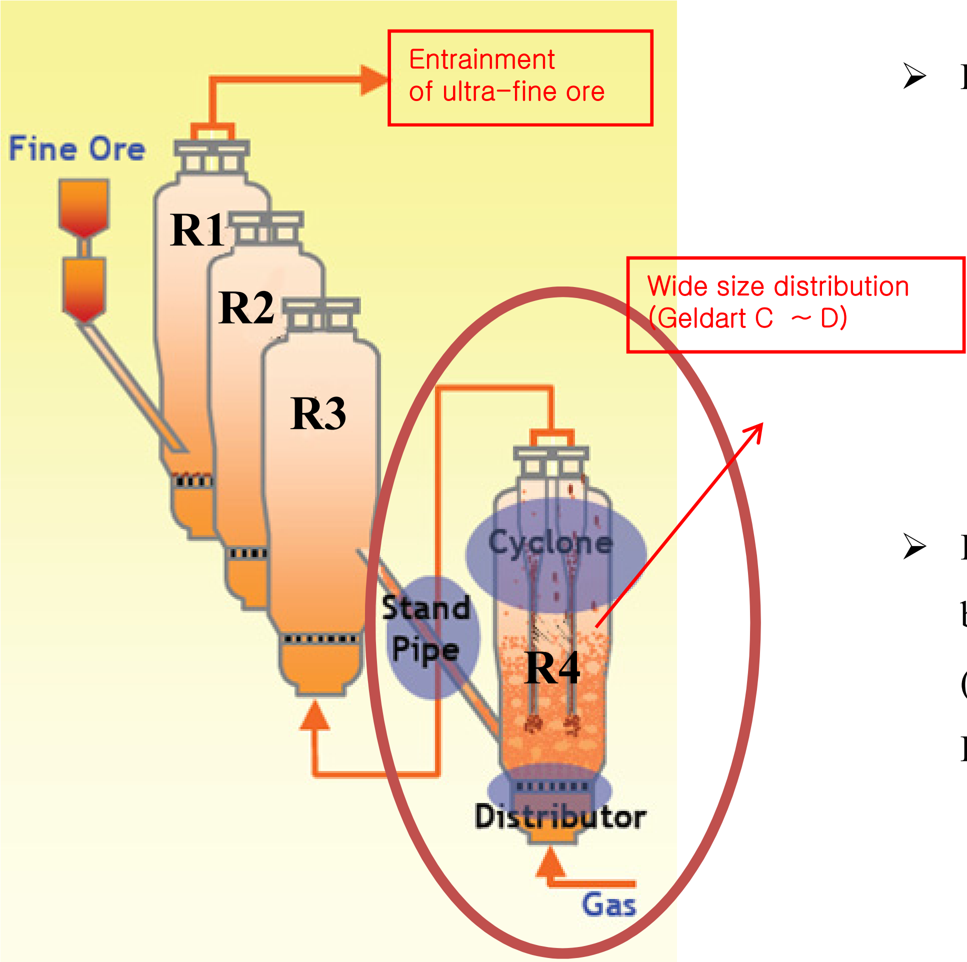

- ➢ POSCO FINEX process
  - ➢ By using powdered iron ore without preprocessing, it could significantly reduce capital investment costs and pollutant emission
  - ➢ Use almost all particle size range

- ➢ In commercial scale, natural ore particles could be broken down by the high velocity of the distributor. (Werther and Xi, 1993; Xiao *et al*. (2011); Hao *et al*. (2015); Zhang *et al*. (2016)

2. Theory-1

•Attrition sources in fluidized beds

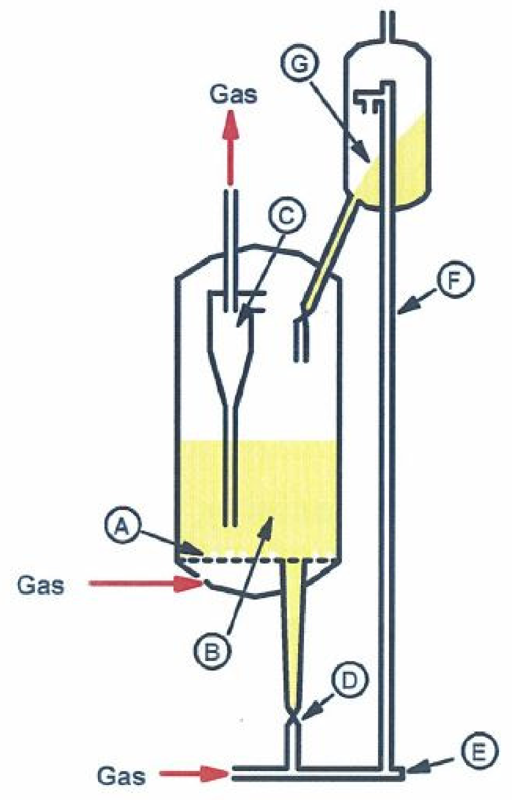

Fig. Sources of attrition in fluid bed systems; PSRI (2011)

- **A. Submerged jet attrition at the grid**
- **B. Bubble attrition**
- **C. Attrition in cyclones**
- D. Attrition at valves of screw feeder
- E. Attrition at elbows
- F. Attrition in dilute-phase pneumatic conveying
- G. Free fall attrition
- Main attrition source in fluidized bed
  - Grid jets, bubbling fluidized bed, cyclones

    Pell (1990); Yang (2003)

2. Theory-2

• **Particle attrition mode in fluidized beds**

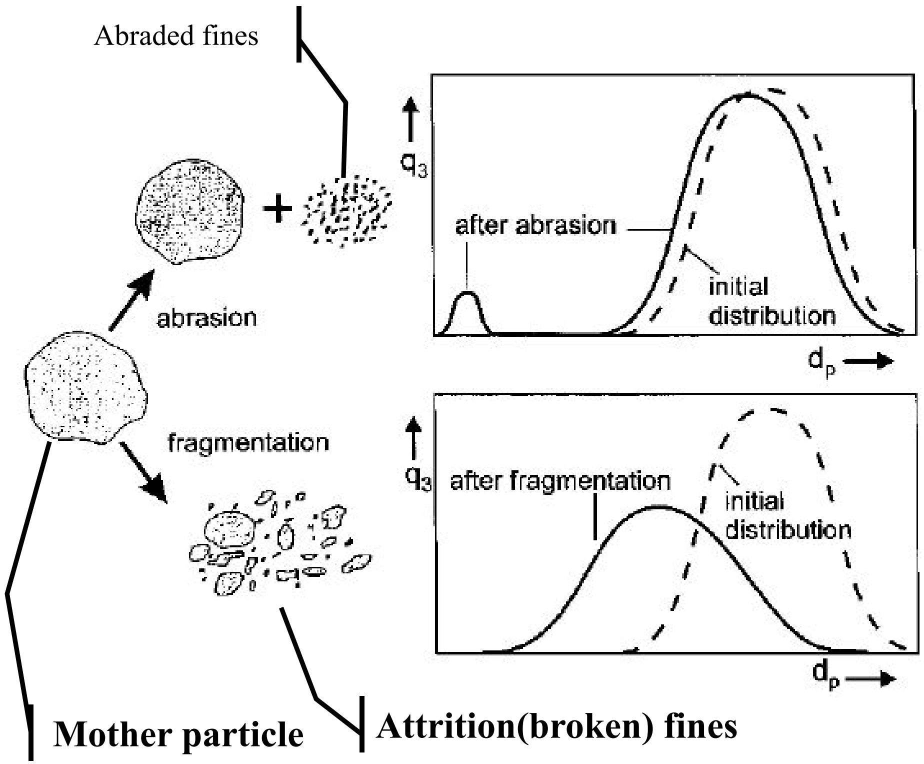

Fig. Attrition modes and their effects on particle size distribution; Yang (2003)

- Abrasion (surface abrasion, wear)
  - Removing the asperities at the particle surface
  - Abraded fines large amount of generation
  - No significant change in the particle size distribution
  - The particle shape goes to round form
  - **Required less energy**
- Fragmentation (breakage)
  - Broken into a number of parts in similar size
  - Increasing in the number of particles
  - Great change in the particle size distribution ($d_{sv}\downarrow$)
  - Pointed out as a primary mechanism causing attrition McMillan et al. (2007)
  - **Required more energy**

SUNG KYUN KWAN UNIVERSITY

2. Theory-3

• Driving force of attrition at air jets

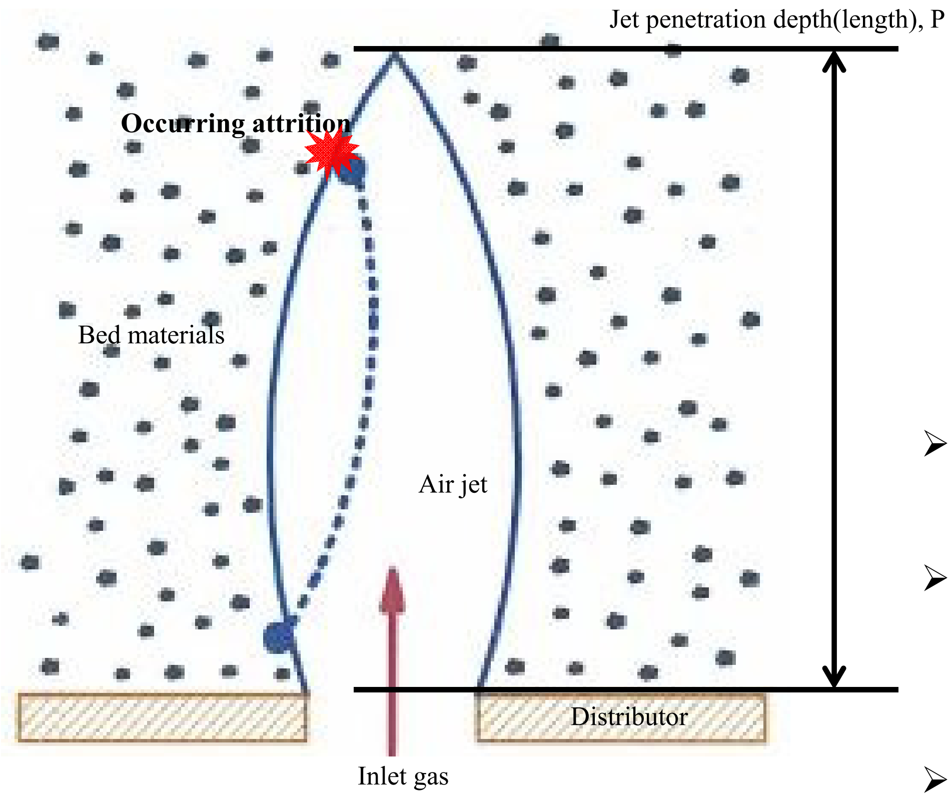

Fig. particle attrition at grids from PSRI (2011)

- **Impact force** has been pointed out as a major driving force in grid jet attrition caused by a **collision** when there bed material flow into the air jet area return to the fluidized bed
  - Bemrose and Bridgwater (1987)
  - Kutyavina and Baskakov (1972)
  - Choi *et al*. (2010)
- Inter-particle impact velocity in fluidized bed grid jet or spout bed is very high, so severe attritions were induced.
- If the bed height is lower than jet penetration length, attrition characteristics could not be easy to treat.
  - Yang (2003)
- At lower part of beds, fragmentation caused by fast particle collision by grid jet occurs
  - Vaux (1978)

2. Theory-4

• **Previous study; kinetic energy rate from orifice - Werther and Xi model (1993)**

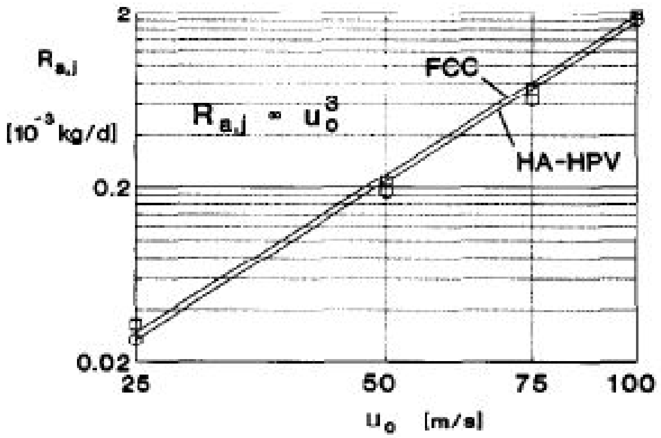

Fig. Influence of jet velocity u_0 on the attrition rate ($d_t = 0.05$ m, unit A, $d_o = 2$ mm, $u = 0.2$ m s^{-1}, u_{pp} variable; □, FCC; ○, HA-HPV).

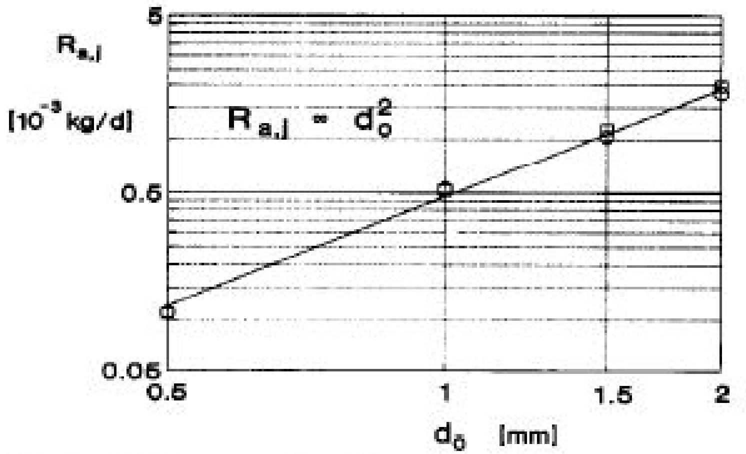

Fig. Influence of orifice diameter d_o on jet attrition rate ($d_t = 0.05$ m, unit A, $u_o = 100$ m s^{-1}, $u = 0.2$ m s^{-1}, u_{pp} variable; □, FCC; ○, HA-HPV).

- In range of jet velocity, u_{or}<100 m/s, the attrition rate was proportional to the cube of the jet velocity
- In range of orifice diameter, 0.5 mm<d_{or}< 2 mm, the attrition rate was proportional to the square of the orifice size.
- Thus, Werther and Xi suggested that the attrition model with kinetic energy rate could be determined as follows:

$$R[\text{fine gen./time}] = K\rho_g {d_{or}}^2 {u_{or}}^3 \propto E_K \quad \text{(Werther and Xi attrition model)}$$

where K [s^2/m^2] is attrition proportional constant, ρ_g [kg/m^3] is a gas density

3. Objective

To investigate the attrition rate of iron ores by air jet

with the variation of the kinetic energy rate from distributor

4. Experiment-1

• Apparatus (no circulation)

➢ Due to using 1 hole gas distributor, particles were inserted during aeration in order to prevent weeping

➢ Elutriation fines were accumulated or collected in the bag house and dipleg through the cyclone

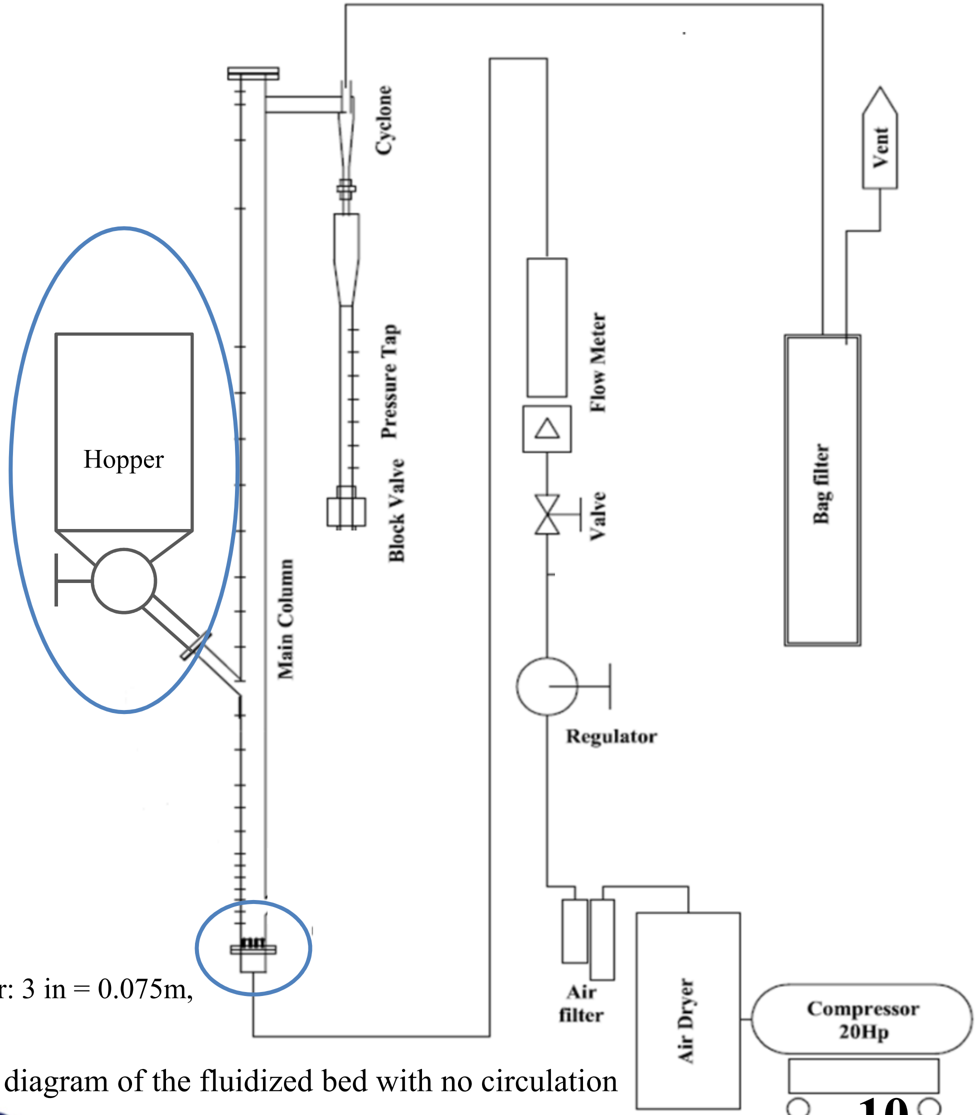

Riser diameter: 3 in = 0.075m,
Height: 3.7 m

Fig. Schematic diagram of the fluidized bed with no circulation

4. Experiment-2

- **Apparatus and procedure (circulation)**

1. Charging the hopper and the loopseal as follows

   Bed inventory: 3.5 or 5.0 kg (-10 mm, sinter100%)

   loopseal inventory 2.5 kg (- 250 µm, sinter 100%)

2. Starting the aeration and checking the circulation
3. Opening the valve of hopper (beginning)
4. Stop the aeration (end, after 30 mins)
5. Screening the all particles (6.0 or 7.5 kg) and then

   calculating the attrition rate

   (bed, loopseal, bag house)

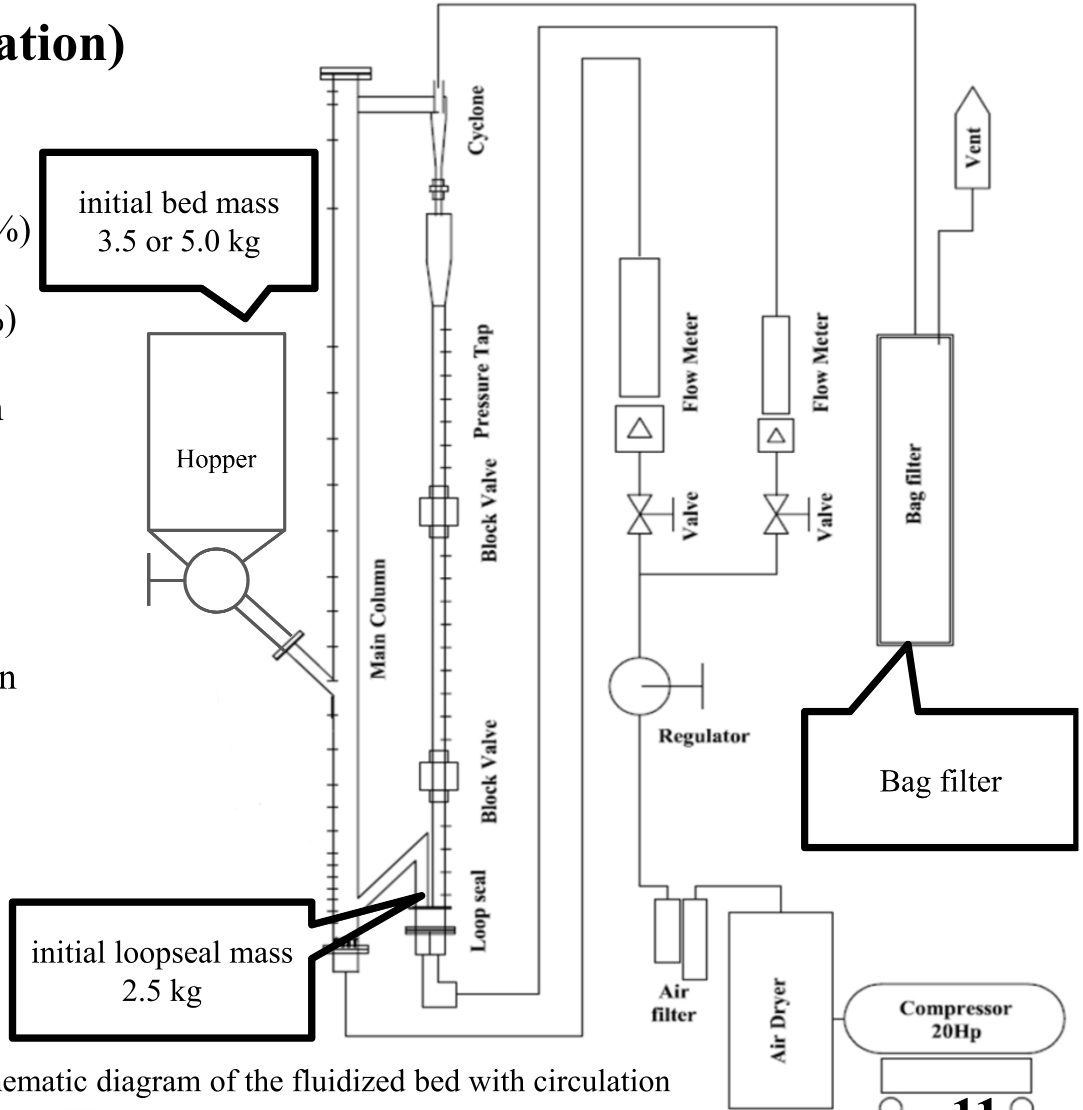

Fig. Schematic diagram of the fluidized bed with circulation

SUNG KYUN KWAN UNIVERSITY

Riser diameter: 3 in = 0.075m,
Height: 3.7 m

4. Experiment-3

• **Apparatus (distributors)**

➢Single hole distributors were used to prevent jet interactions.

➢Designing orifice nozzle diameter with air jet velocity, 113 m/s(nearly commercial nozzle velocity)

➢ $\frac{\pi}{4} D_t^2 U_g = \frac{\pi}{4} d_{or}^2 u_{or} = Q(\text{volume flow rate})$ $(D_t = 3\text{in},, d_{or}, u_{or} = 113\text{m/s})$

➢$\dot{m} = \rho_g A_{or} u_{or} = \rho_g \frac{\pi}{4} d_{or}^2 u_{or} = 0.0068 \text{ kg/s}$ $(\rho_g = 1.2 \text{ kg/m}^3)$

➢$\therefore \dot{\mathbf{E}}_{\mathbf{K}} = \frac{\mathbf{1}}{\mathbf{2}} \dot{\mathbf{m}} \mathbf{u}_{\mathbf{or}}^{\mathbf{2}} = \mathbf{43} \text{ J/s}$

$U_g = 1.2 \text{ m/s}$ ▶ $d_{or} = 0.0080\text{m} = \mathbf{8.0\ mm}$

$U_g = 2.0 \text{ m/s}$ ▶ $d_{or} = 0.0101\text{m} = \mathbf{10.1\ mm}$

$U_g = 2.5 \text{ m/s}$ ▶ $d_{or} = 0.0113\text{m} = \mathbf{11.3\ mm}$

$U_g = 3.0 \text{ m/s}$ ▶ $d_{or} = 0.0124\text{m} = \mathbf{12.4\ mm}$

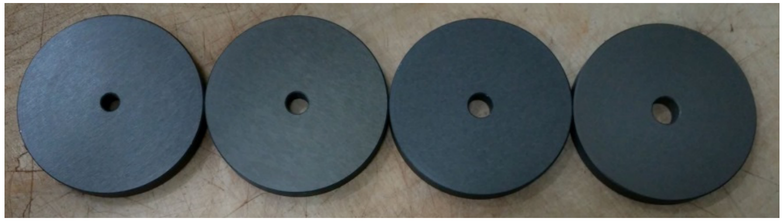

Fig. Designed distributor (8, 10.1, 11.3, and 12.4 mm)

SUNG KYUN KWAN UNIVERSITY

4. Experiment-4

• Experimental condition

Table Kinetic energy rate from orifice with superficial gas velocity and distributor

Condition	U_g [m/s]	u_{or} [m/s]	d_{or} [mm]	m_g [kg/s]	E_K [J/s]	Time [min]	Mass basis [kg]	
							column	loopseal
No circulation	1.25	113	8	0.0068	43.9	30	3.5	0
No circulation	2.50	94	12.4	0.0137	60.9	30	3.5	0
No circulation	2.25	102	11.3	0.0123	64.4	30	3.5	0
No circulation	2.00	113	10.1	0.0109	70.9	30	3.5	0
No circulation	2.75	104	12.4	0.0150	81.1	30	3.5	0
No circulation	2.50	113	11.3	0.0137	88.4	30	3.5	0
No circulation	2.25	128	10.1	0.0123	100.9	30	3.5	0
No circulation	3.00	113	12.4	0.0164	105.3	30	3.5	0
No circulation	2.75	125	11.3	0.0150	117.6	30	3.5	0
No circulation	2.50	142	10.1	0.0137	138.5	30	3.5	0
No circulation	3.00	136	11.3	0.0164	152.8	30	3.5	0
No circulation	2.00	181	8	0.0109	**180.2**	30	3.5	0
No circulation	2.75	156	10.1	0.0150	**184.4**	30	3.5	0
No circulation	3.00	171	10.1	0.0164	**239.4**	30	3.5	0
No circulation	2.25	204	8	0.0123	**256.5**	30	3.5	0
No circulation	2.50	227	8	0.0137	**351.9**	30	3.5	0
No circulation	3.00	272	8	0.0164	**608.1**	30	3.5	0
No circulation	3.00	272	8	0.0164	608.1	300	2.5	0
Circulation	2.00	181	8	0.0109	**180.2**	30	3.5	2.5
Circulation	2.25	204	8	0.0123	**256.5**	30	3.5	2.5
Circulation	2.50	227	8	0.0137	**351.9**	30	3.5	2.5
Circulation	3.00	272	8	0.0164	**608.1**	30	3.5	2.5
Circulation	2.50	227	8	0.0137	**351.9**	30	**5.0**	2.5
Circulation	3.00	272	8	0.0164	**608.1**	30	**5.0**	2.5

Standard ASTM method:

no circulation; U_g=0.17 m/s;

u_{or}=448 m/s; d_{or}=0.397 mm;

E_K= 6.7*3 = **20.1 J/s**

SUNG KYUN KWAN UNIVERSITY

4. Experiment-5

- **Particles (fresh sinter feed of iron ore)**

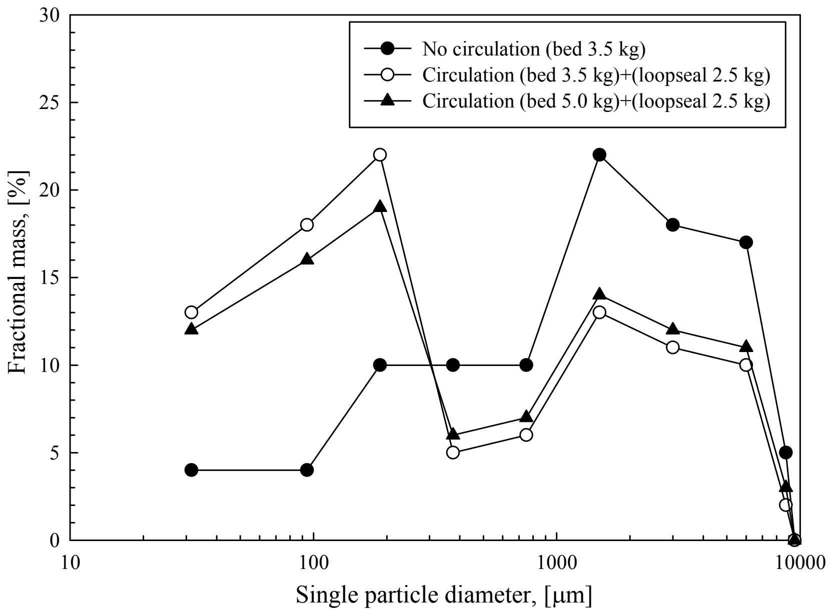

Fig. Fractional mass of bed materials

Table Particle size distribution of bed materials (feed)

Range [μm]	Average diameter [μm]	Fractional mass [%]			
		No circulation (3.5 kg basis)	Circulation (6.0 kg basis)	Circulation (7.5 kg basis)	Loopseal (2.5 kg basis)
		3.5(bed)	3.5(bed)+2.5	5.0(bed)+2.5	0(bed)+2.5
0 – 63	31.5	4	13	12	26
63 – 125	94	4	18	16	36
125 – 250	187.5	10	22	19	38
250 – 500	375	10	5	6	0
500 – 1000	750	10	6	7	0
1000 – 2800	1500	22	13	14	0
2800 – 4750	3000	18	11	12	0
4750 – 8000	6000	17	10	11	0
8000 – 9500	8750	5	2	3	0
d_P		357	133	152	71

Table Density of bed material

Material	True density[kg/m^3]
Sinter feed	3,705

5. Result and Discussion-1

• **Threshold size of attrition fine with no circulation**

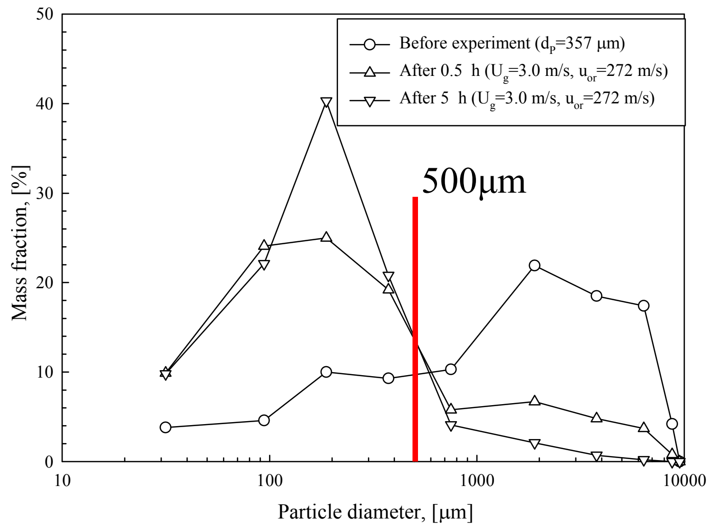

Fig. Mass fractions between before and after experiments

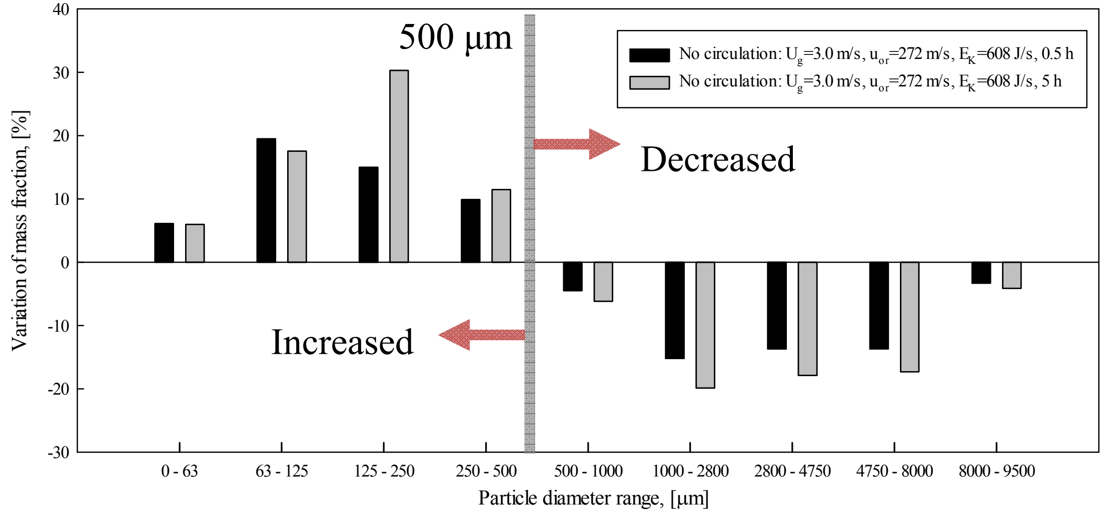

Fig. Zenz and Kelleher bar; the differences of mass fraction between before and after experiments

Zenz and Kelleher(1980)
$y = (x_{after} - x_{before})$
$x: mass\ fraction$

- ➢ Variation of particle size distributions before and after the experiment intersected at 500 μm in the severest condition U_g = 3.00 m/s, u_{or} = 272.2 m/s, E_k = 608 J/s, 0.5 hour
- ➢ It is reasonable to determine the threshold size of attrition fine as 500 μm.

5. Result and Discussion-2

• Attrition trend with the kinetic energy rate

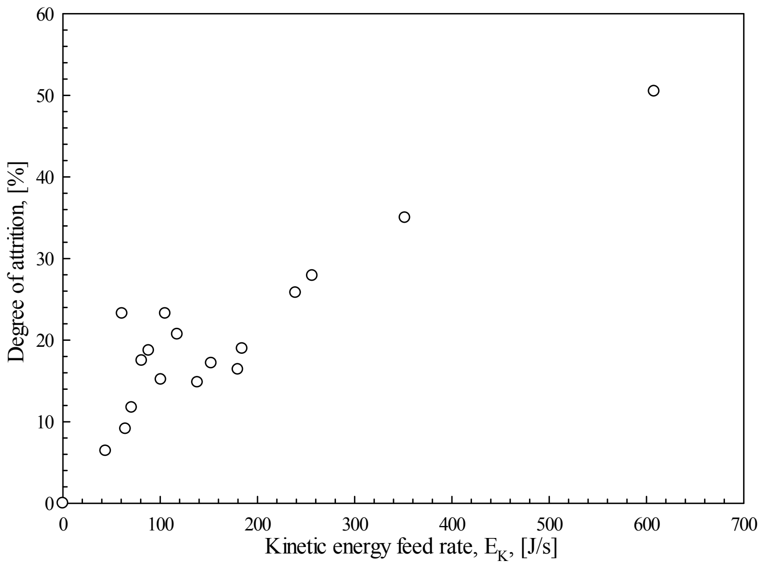

Fig. Degree of attrition with kinetic energy rate

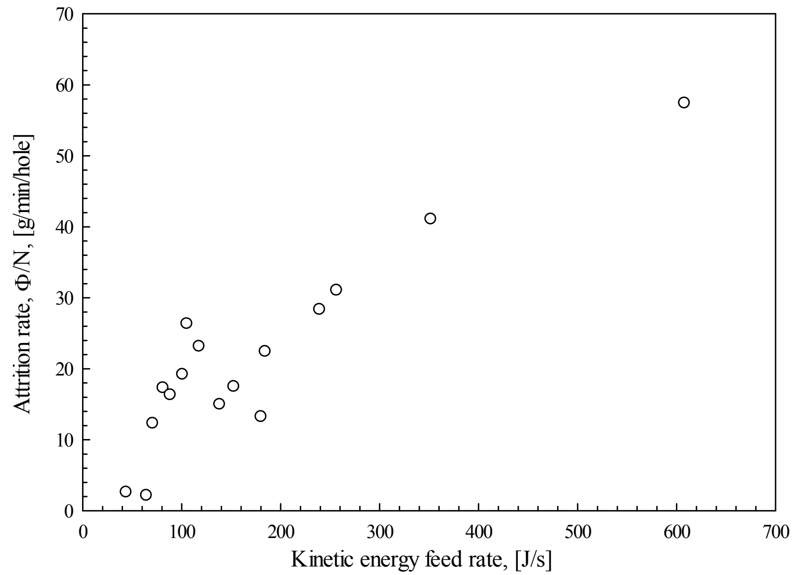

Fig. Attrition rate with kinetic energy rate

- ➢ Attrition trends were not clear in the range E_K<180 J/s.
- ➢ Attrition rates increased with increasing the kinetic energy rate from orifice clearly in the range $E_K \geq 180$ J/s corresponded with Werther and Xi attrition model (1993)

$$\text{Degree of attrition\%} = \frac{\sum M_{d_P\ \mathrm{end}} - \sum M_{d_P,\mathrm{ini}}}{M_{\mathrm{ini}}} \cdot 100 = \sum (x_{d_p,\mathrm{end}} - x_{d_p,\mathrm{ini}}) \cdot 100$$

Ray and Jiang, 1987

5. Result and Discussion-3

- **Variation of size distribution with no circulation ($E_K \geq 180$ J/s)**

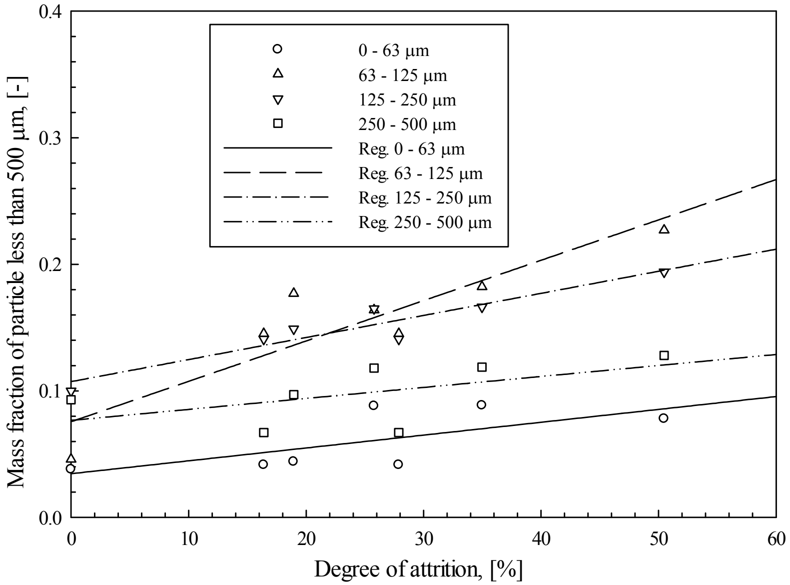

Fig. The mass fraction of each no circulation experiments with degree of attrition; (attrition fines)

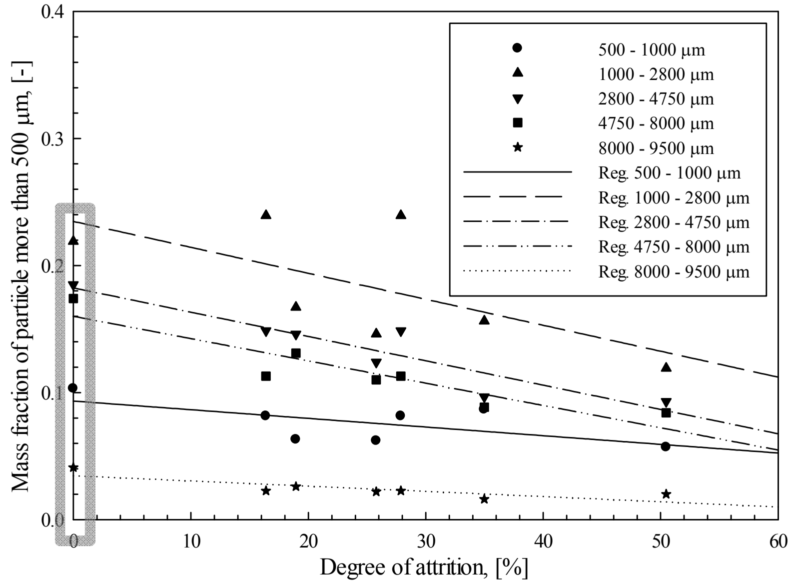

Fig. The mass fraction of each no circulation experiments with degree of attrition; (mother particles)

- Fractional masses were varied with following regression lines during fixed 30 mins attrition time.
- Zhang et al. (2016) reported that the attrition rates could be calculated by the variation of mother particle size distribution.
- The error between y-intercept and y value were regarded as "initial attrition".
- The effect of "initial attrition" could be ignored.

Ray and Jiang (1987)

$$\text{Degree of attrition\%} = \frac{\sum M_{d_p\,\text{end}} - \sum M_{d_p,\text{ini}}}{M_{\text{ini}}} \cdot 100 = \sum (x_{d_p,\text{end}} - x_{d_p,\text{ini}}) \cdot 100$$

5. Result and Discussion-4

- **Threshold size of attrition fine with circulation ($E_K \geq 180$ J/s)**

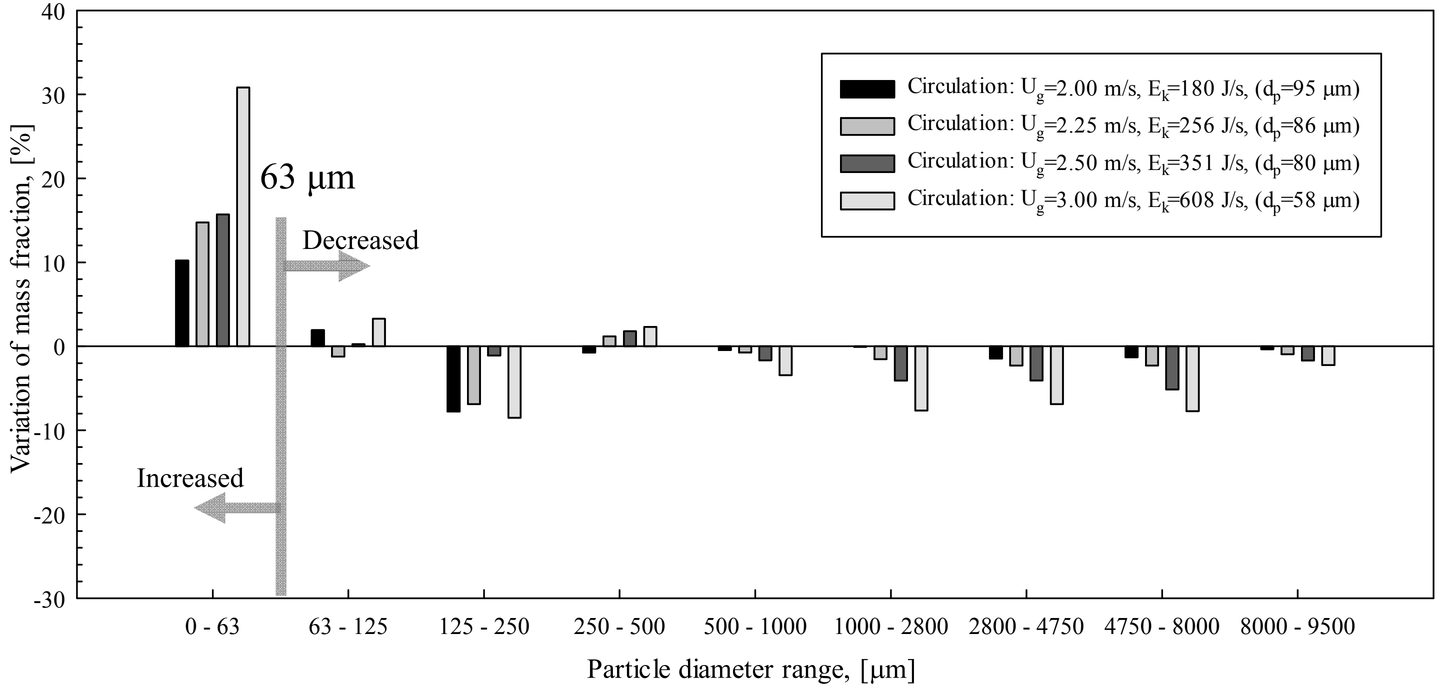

Fig. The differences of mass fraction between before and after experiments

- The particles less than 63 μm increased significantly unlike no circulation.
- It is reasonable that threshold size of attrition fines should be shifted to 63 μm

Zenz and Kelleher(1980)
$y = (x_{after} - x_{before})$
$x: mass\ fraction$

5. Result and Discussion-5

- **Experimental static bed height with theoretical jet length ($E_K \geq 180$ J/s)**

Table Theoretical jet length and experimental bed heights in range of $E_K \geq 180$ J/s

Condition	U_g [m/s]	u_{or} [m/s]	d_{or} [mm]	E_K [J/s]	Mass basis [kg]		Experimental static bed height* [cm]	Theoretical jet length [cm]
					column	loopseal		
No circulation	2.00	181	8	180.2	3.5	0	**23.1**	19.2
No circulation	2.75	156	10.1	184.4	3.5	0	19.5	21.7
No circulation	3.00	171	10.1	239.4	3.5	0	16.4	22.7
No circulation	2.25	204	8	256.5	3.5	0	17.3	20.3
No circulation	2.50	227	8	351.9	3.5	0	13.9	21.5
No circulation	3.00	272	8	608.1	3.5	0	6.5	23.5
Circulation	2.00	181	8	180.2	3.5	2.5	**30.1**	21.1
Circulation	2.25	204	8	256.5	3.5	2.5	**27.0**	22.4
Circulation	2.50	227	8	351.9	3.5	2.5	**27.3**	23.7
Circulation	3.00	272	8	608.1	3.5	2.5	20.9	25.9
Circulation	2.50	227	8	351.9	5.0	2.5	**26.7**	23.4
Circulation	3.00	272	8	608.1	5.0	2.5	**25.6**	25.6

)*: Experimental static bed heights were calculated by the bed weight after experiments

- At the ends of the each experiments, the bed heights should be higher than the each jet penetration lengths.
- Instead of the fluidized bed height, the static bed heights were compared with the jet lengths.
- According to Werther and Xi (1993), the attrition rates with higher bed heights than jet lengths were constant regardless of the bed inventory or the bed height.

5. Result and Discussion-6

• Attrition rates of iron ore with the kinetic energy rates

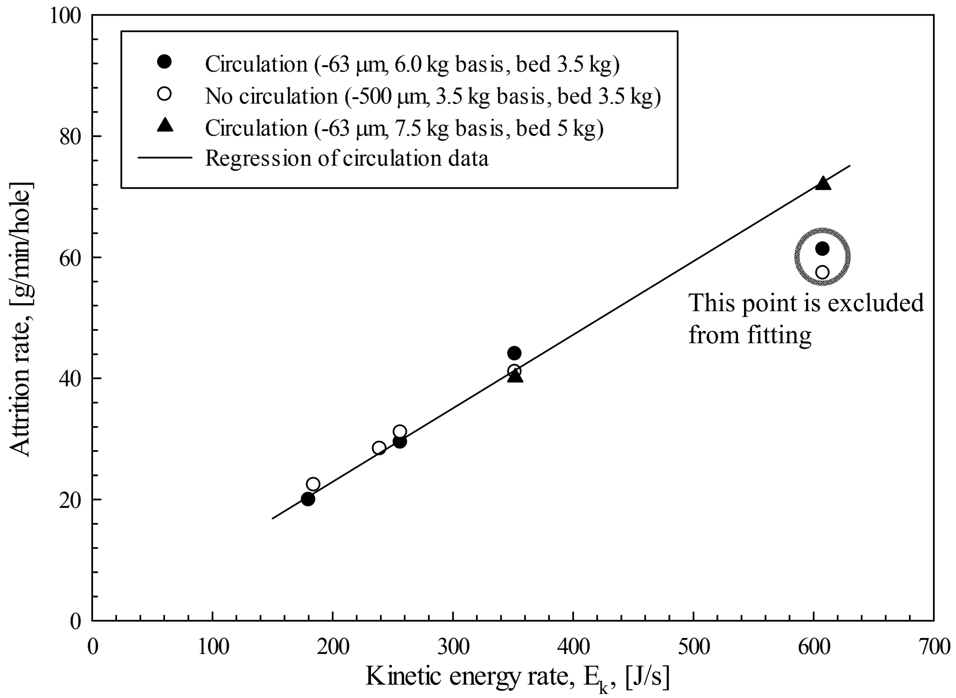

Fig. Attrition rate with kinetic energy rate from orifice in range $E_K \geq 180$ J/s (data regression with ● and ▲)

- Attrition rates of iron ore increased with increasing the kinetic energy rates in the range $E_K \geq 180$ J/s.
- Fragmentation dominant trends were observed entirely.
- Werther and Xi (1993) attrition model was still valid in spite of occurring many fragmentations.
- When the bed height was lower than jet length, the attrition rate did not follow the existing trend.

Linear regression

$$\Phi/N = 0.1214E_K - 1.3587$$

$$(180 \text{ J/s} \leq E_K \leq 608 \text{ J/s})$$

where N is the number of orifice[hole], Φ is the attrition rate [g/min]

6. Conclusion

1. Attrition rates of the iron ore with kinetic energy rate from orifice by varying the sizes of single orifice and the superficial gas velocity were investigated in the range 180 J/s ≤ E_K ≤ 608 J/s.

2. The threshold size of attrition fines could be determined as "500 μm" with no circulation and "63 μm" with circulation.

3. With no circulation, the experimental range, E_K ≥ 180 J/s which indicated the definite attrition trend was observed.

4. Werther and Xi (1993) attrition model was still valid in spite of occurring many fragmentations.

5. With circulation, the attrition correlation was obtained as $\Phi/N = 0.1214E_K - 1.3587$ in the given range.

Thank you for your attention.

SUNG KYUN KWAN UNIVERSITY

Appendix

- **Reference of CO2 capturing by limestone**

*G. Xiao, J.R. Grace, C.J Lim, *Powder Technology*, **Vol. 207**, 2011, 183 – 191
"Attrition characteristics and mechanisms for limestone particles in an air-jet apparatus"

*P. Sun, J.R. Grace, C.J. Lim, E.J. Anthony, *AIChE*, **Vol. 53**, 2007, 2432 - 2442
"The effect of CaO sintering on cyclic CO2 capture in energy system"
'Limestone is widely used as a sorbent in fluidized beds, especially for SO2 and CO2 capture, because of its low price and wide availability.'

*P. Sun, J.R. Grace, C.J. Lim, E.J. Anthony, *Environ. Sci*. Technol. **Vol. 41**, 2007, 2943 – 2949
"Sequential capture of CO2 and SO2 in a pressurized TGA simulating FBC conditions"

*R. Pacciani, C.R. Müller, J.F. Davidson, J.S. Dennis, A.N. Hayhurst, *AIChE*, **Vol. 54**, 2008, 3308 – 3311
"How does the concentration of CO2 affect its uptake by a synthetic ca-based solid sorbent?"

*J.C. Abanades, E.J. Anthony, D.Y. Lu, C. Salvador, D. Alvarez, *AIChE*, **Vol. 50**, 2004, 1614 – 1622
"Capture of CO2 from combustion gases in a fluidized bed of CaO"

Appendix (earlier studies)

Authors	Correlation	Variable	Etc.
Forsythe and Hertwig, 1949	$R[\%/hr] = \frac{(x_{fine\ after\ 1h} - x_{fine\ at\ start})}{(x_{nonfine\ at\ start})} \times 100$	Time: 1 h	FCC Fine threshold: 44, 40, 20 μm
Gwyn, 1969	$R[kg/h] = \frac{dW}{dt} = knt^{n-1}$		FCC All elutriated fines
Haase et al., 1975 Alcan International, 1982	$R[\%/hr] = \frac{(x_{fine\ after\ 1h} - x_{fine\ at\ start})}{(x_{nonfine\ at\ start})} \times 100$	Time: 1 h	Fine threshold: 45 μm
Lin et al., 1980 Kono, 1981	$R[\%/hr] = \frac{(x_{fine\ after\ 1h} - x_{fine\ at\ start})}{(x_{nonfine\ at\ start})} \times 100 = k$	No time-dependence	
Chen et al., 1980	$R[kg/h] = CS\frac{\rho_g Q(\beta u_{or})^2}{W d_P \rho_P}$	u_{or}=25-300 m/s	Iron ore (142-274 μm, 3940 kg/m^3)
Zenz and Kelleher, 1980	$R[kg/h] = C\left(u_{or}\sqrt{\rho_g}\right)^{2.5} \pi d_{or}{}^2/4$	u_{or}=33-303 m/s	Silica-alumina FCC
Werther and Xi, 1993	$R[kg/h] = C\rho_g d_{or}{}^2 u_{or}{}^3 \propto E_K$	u_{or}=25-100 m/s	FCC (106 μm, 1500 kg/m^3)
Ghadiri et al., 1994	$R[kg/h] = Cd_{or}{}^n u_{or}{}^m$	u_{or}=25-125 m/s FCC; n= 0.6-0.76, m=3.31 NaCl; n=0.44-1.11, m=5.1	FCC(425-600 μm) NaCl(90-106 μm)
McMillan et al., 2007	$\eta = 7.81 \times 10^{-7} \alpha\beta d_{or}{}^{1.131} u_{or}{}^{0.55} (\rho_g u_{or}{}^2)^{1.635} \left(\frac{u_g - u_{mf}}{u_{mf}}\right)^{0.494}$		Grinding efficiency, η[m^2/kg] Sonic nozzle
ASTM D5757, 2011	$R[\%] = \frac{m_{fine\ after\ 5h}}{m_{bed}} \times 100$	Time: 5 h	All elutriated fines
PSRI, 2011	$\Phi/N\left[\frac{g}{min \cdot hole}\right] = \frac{m_{fine}}{t \cdot N_{or}}$		Fine threshold: d_P